Dynamics and Microstructure Formation during Nucleation of Lysozyme Solutions

Yannis Georgalis,*,‡ Patrick Umbach,‡ Dikeos Mario Soumpasis,† and Wolfram Saenger‡

Contribution from the Institut für Kristallographie Freie Universität Berlin, Takustrasse 6, 14195 Berlin, and Biocomputation Group, Max-Planck-Institut für Biophysikalische Chemie, P.O. Box 28141, 37018 Göttingen, Germany

Received October 17, 1997

Abstract: The liquid−liquid coexistence region of aqueous lysozyme−NaCl solutions was examined by time-resolved small-angle static light scattering and light microscopy. At the initial stages of the reaction scattered intensities peaked at finite scattering vectors as expected for globular domains growing under the influence of competing interactions. An oscillatory behavior of the mean domain radius is observed at later stages of the reaction as a function of time. Microscopic observations revealed domains undergoing correlated ripening with time and forming labyrinthine microstructure and microcrystals at later stages. Potentials of the mean force computations yield first qualitative insights into the effective pair interactions during the process. The behavior of the system can be understood qualitatively as spinodal decomposition followed by nucleation, leading to a modulated phase type of microstructure.

Introduction

The prediction of optimal protein crystallization conditions is the major obstacle in obtaining three-dimensional structures of biomolecules at atomic resolution. Studies of aggregation which accompanies nucleation in supersaturated protein solutions, by scattering techniques, has become an actual research topic. The increasing use of light scattering techniques has led to interesting, but not always convergent, results. Several investigations concerning these topics have been recently reviewed in ref 1. Cumulative research reports can be found in the following: *J. Crystal Growth* **1991** *110*; **1992**, *122*, and *Acta Crystallogr Sect. D* **1994**, *50(4)*.

Despite rapid, and by far more conclusive, progresses in the crystallization of colloids,[2−4] protein crystallization follows only "asymptotically" these research trends, a shortcoming mainly because protein crystallization is heterogeneous. The field, as such, is therefore still lacking a rigorous physicochemical background and relies solely on empirical recipes for determining appropriate crystallization conditions. Supersaturated solutions of proteins do not crystallize unless proper charge screening and packing conditions are met. For simple systems such as ionic salts, the degree of supersaturation may serve as a convenient measure. However, with proteins, requirements for maintaining the active ("native") state and interactions with the solvent do not allow for such simplified considerations.

In a series of publications[5−8] we have identified conditions for the system lysozyme−NaCl based on the study of fractal (amorphous precipitate) microstructure formed at volume fractions below $\varphi < 0.10$ (taking the radius of the lysozyme monomer to be 1.92 nm). The cluster formation observed in our kinetic studies was also verified by other investigators[9,10] using small-angle neutron and light scattering.

Liquid−liquid and liquid−solid phase separation for the lysozyme−NaCl system have been very recently investigated.[11,12] A comparison of phase diagrams[11] has shown that a competition may occur between liquid−liquid and liquid−solid transitions, giving rise to a variety of instabilities. We have undertaken a study of these events by extending our previous observations to volume fractions $0.10 < \varphi < 0.20$, typical for observing the phase separation. For these studies we have employed time-resolved small-angle static light scattering (SLS) and video-assisted high resolution optical microscopy. The experiments described below differ from those reported in our previous works, under isothermal supersaturation conditions, in the sense that phase separation is here promoted by temperature quenches.

Brief Theory

Light Scattering. Light scattering is a convenient technique for studying systems exhibiting structural organization on length

* To whom correspondence should be addressed. Tel: ++4930-838-4588. FAX: ++4930-838-6702. E-mail: yannis@chemie.fu-berlin.de.

† Max-Planck-Institut für Biophysikalische Chemie.

‡ Institut für Kristallographie Freie Universität Berlin.

(1) Giegé, R.; Drenth, J.; Ducruix, A.; McPherson, A.; Saenger, W. *Prog. Crystal Growth Charact.* **1995**, *30*, 237.

(2) Pusey, P. N. *Colloidal Suspensions in Liquids, Freezing Glass Transition*; Hansen, J. P., Levesque, D., Zinn-Justin, J., Eds.; Elsevier: Amsterdam, 1991; p 765.

(3) Poon, W. C. K.; Pusey, P. N. In *Observation, Prediction and Simulation of Phase Transitions in Complex Fluids*; Baus, M., et al., Eds.; Kluwer: Netherlands, 1995; p 3.

(4) Ackerson, B. J.; Schätzel, K. *Phys. Rev. E* **1995**, *52(6)*, 6448.

(5) Georgalis, Y.; Zouni, A.; Eberstein, W.; Saenger, W. *J. Crystal Growth* **1993**, *126*, 245.

(6) Saenger, W.; Georgalis, Y. *Adv. Colloid Interface Sci.* **1993**, *46*, 165.

(7) Georgalis, Y.; Schüler, J.; Frank, J.; Soumpasis, M. D.; Saenger, W. *Adv. Colloid Interface Sci.* **1995**, *58*, 57.

(8) Umbach, P.; Georgalis, Y.; Saenger, W. *J. Am. Chem. Soc.* **1998**, *120*(10), 2382.

(9) Niimura, M.; Minezaki, Y.; Ataka, M.; Katsura, T. *J. Crystal Growth* **1995**, *154*, 136.

(10) Tanaka, S.; Yamamoto, M.; Kawashima, K.; Ito, K.; Hayakawa, R.; Ataka, M. *J. Crystal Growth* **1996**, *168*, 44.

(11) Tanaka, S.; Yamamoto, M.; Ito, K.; Hayakawa, R.; Ataka, M. *Phys. Rev. E* **1997**, *56(1)*, R67.

(12) Muschol, M.; Rosenberger, F. *J. Chem. Phys.* **1997**, *107(6)*, 1953.

S0002-7863(97)03614-7 CCC: $15.00
Published on Web 05/21/1998

scales comparable to those of the wavelength of the incident light.[13] The technique measures the interference between light scattered by different points in the sample. The spatial resolution is determined by the scattering vector, **q**, whose magnitude is given by the Bragg condition:[14]

$$q = \frac{4\pi n}{\lambda} \sin(\theta/2) \tag{1}$$

Here, λ denotes the wavelength of the scattered light *in vacuo*, n the refractive index of the solvent, and θ the scattering angle. The vectors of the incident and scattered light define virtual fringe planes with spacing which is associated with the average distance R of the scatterers:

$$R = \frac{\pi}{q} \tag{2}$$

For a given scattering vector, pairs of points separated by a distance less than R, scatter light which is in phase and these contributions can be lumped together. This gives rise to interference patterns determined by the relative contents of small volumes of the order R^3. If the sample is homogeneous, all these volumes have the same mass and their contributions will cancel in the interference process. The examined sample will then be transparent; otherwise, the cancellation will be incomplete and scattering will occur.

Phase Separation. When a system is suddenly quenched to temperatures within the unstable region in the phase diagram, a phase separation is expected to occur. The homogeneous phase is no longer stable, and phases with different concentrations will form via concentration fluctuations with distinct wavelengths.[15,16]

Figure 1A shows a simplified phase diagram in the temperature-density plane. The binodal (coexistence) line gives the equilibrium compositions after separation, and the spinodal line separates the biphasic region to a metastable and an unstable region.[17] Below the spinodal line, the system is unstable, and phase separation will occur spontaneously without an activation barrier. Here, the system exhibits an instability against small-amplitude, long wavelength (λ_c), delocalized concentration fluctuations known as spinodal decomposition (SD). When the system crosses into the metastable region, an activation barrier has to be surmounted, to form phases with different concentrations (nucleation). Here, the system exhibits an instability against large-amplitude (R_c), localized concentration fluctuations of the new phase in the bulk.[18] A pictorial representation of these events is shown in Figure 1B.

Spinodal Decomposition. The decay of concentration fluctuations after a system has been quenched into the unstable region is known as spinodal decomposition (SD).[19−21] Transparent and compact descriptions of the lengthy SD theory have been given by Rouw et al.[22] and more recently by Dhont.[23,24] The theory is based on spatiotemporal variations of the local excess concentration $\mu(\mathbf{r}, t) = \rho(\mathbf{r}, t) - \bar{\rho}$, $\rho(\mathbf{r}, t)$ being the local number density at time t and $\bar{\rho}$ the equilibrium concentration of the homogeneous system. The quantity $\mu(\mathbf{r}, t)$ is the order parameter of the system. Small-angle SLS measures μ, averaged over the scattering volume, when the scattering vector q approaches 0. The order parameter is termed conserved when the small-angle scattered intensity approaches zero, while being independent of time, and nonconserved otherwise [See also ref 25 for more details on definitions.].

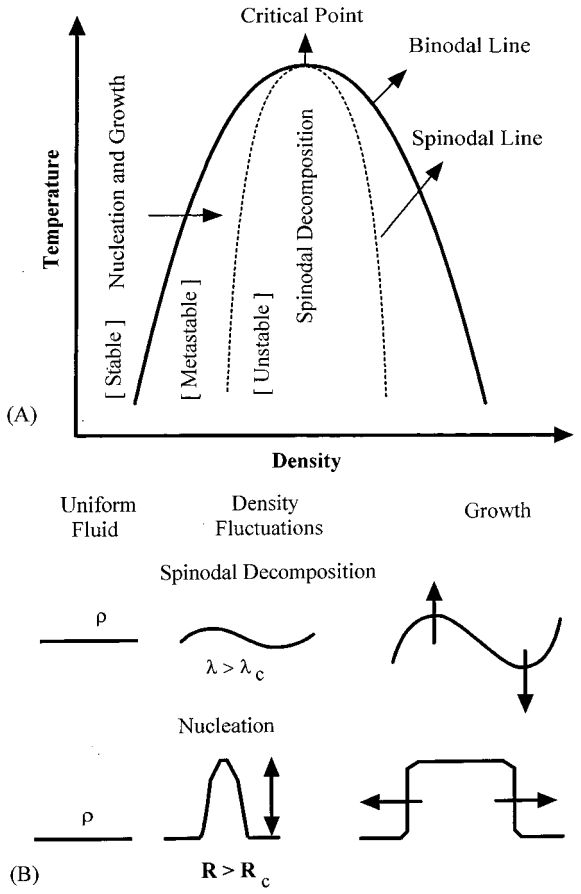

Figure 1. (A) Hypothetical phase diagram in the temperature-density plane. The full line denotes the binodal and the dashed line the spinodal regions, respectively. Below the spinodal line the system is unstable; between binodal and spinodal lines it is confined to the metastable region where the system decays via nucleation and growth. (B) Schematic representation of the density fluctuations leading to phase transition in the unstable region following an SD mechanism (top) or in the metastable region by nucleation (bottom), modified from refs 41 and 16.

When SD is examined by light, or other scattering techniques, an intensity peak is observed. This peak is localized at a scattering vector **q** which typifies the dominant fluctuation length (assumed to be inversely proportional to the average linear domain size [Equation 2 is in this case approximately correct due to irregular domain arrangement and fluctuations of the mean domain size.]). This peak moves to smaller scattering vectors, corresponding to larger length scales, as phase separation and concomitant domain growth proceed.

(13) Guenoun, P.; Gastaud, R.; Perrot, F.; Beysens, D. *Phys. Rev. A.* **1987**, *36(10)*, 4876.
(14) Berne, B.; Pecora, R. *Dynamic Light Scattering*; Academic Press: New York, 1976.
(15) Guggenheim, E. A. *Thermodynamics*; North Holland Publishing: Amsterdam, 1967.
(16) Davis, H. T. *Statistical Mechanics of Phases, Interfaces Thin Films*; VCH Publischers: New York, 1996.
(17) Penrose, O.; Lebowitz, J. L. In *Fluctuation Phenomena*; Montroll, E. W., Lebowitz, J. L., Eds.; North Holland: Amsterdam, 1979; p 293.
(18) Gunton, J. D.; San Miguel, M.; Sahni, P. S. In *Phase Transitions and Critical Phenomena*; Domb, C., Lebowitz, L. J., Eds.; Academic Press: New York, 1983; p 267.
(19) Cahn, J. W. *J. Chem. Phys.* **1965**, *42*, 93.
(20) Hilliard, J. E. In *Phase Transformations*; Aronson, H. I., Ed.; American Society for Metals: Metals Park, OH, 1970; Chapter 12.
(21) Cook, H. E. *Acta Metall.* **1975**, *18*, 297.
(22) Rouw, P. W.; Woutersen, A. T. J. M.; Ackerson, B. J.; de Kruif, C. G. *Physica A* **1989**, *156*, 876.
(23) Dhont, J. K. G. *J. Chem. Phys.* **1996**, *105(12)*, 5112.
(24) Dhont, J. K. G. *Progr. Colloid, Polym. Sci.* **1997**, *104*, 66.
(25) Ramakrishnan, T. V.; Yussouff, M. *Phys. Rev. B.* **1979**, *19(5)*, 19.

The use of time-resolved small-angle SLS enables the determination of the structure factor $S(q, t)$, *i.e.*, the Fourier transform of the order parameter fluctuations, to be deduced from time-resolved measurements of the angular dependence of the scattered intensity as

$$I(q, t) \propto S(q, t) \propto \int \langle \mu(0, t)\, \mu(\mathbf{r}, t) \rangle \exp(i\mathbf{qr}) \mathrm{d}^3\mathbf{r} \quad (3)$$

The main feature of pure SD is that the long wavelength diffusion coefficient becomes negative.[19,26] Consequently, growth instead of decay of the fluctuations occurs. Density fluctuations occurring on spatial scales large compared to the characteristic length of the evolving domains give rise to light scattering. Growth can then be observed in regions where the form factors of the domains are constant.

Denoting with $q_m(t)$ the largest scattering vector for which the corresponding peak amplitude attains its half-value, $I_m(t)$, one obtains two useful relations that allow for experimentally assessing different classes of ordering.[27,28] The peak amplitude evolves in time as

$$I_m(t) \sim t^{6m+1} \quad (4)$$

and the characteristic domain radius $R_m(t)$ [$R_m(t)$ corresponds to $q_m(t)$ which is not the scattering vector at the peak maximum.] as

$$R_m(t) \sim t^{1/m} \quad (5)$$

An exponent $m = 2$ suggests a Lifschitz−Allen−Cahn type of kinetics,[29] or if $m = 3$ a Lifschitz−Slyojov[30] of kinetics.[31] These power-laws signify ripening processes where growth is constrained by competition for material among various regions. Linear scaling behavior, $R_m(t) \sim t$, is observed[32] if there is no obvious competition for material. The volume fractions separating those regimes are not predicted by theory.[33] As pointed out[28] continuous coarsening may involve an increment of the exponents typifying $R_m(t)$ between 1/3 and 1/2, or to even higher values at larger volume fractions. Such changes, reflect transitions among various coarsening mechanisms.[34−36]

Nonequilibrium scaling is manifested through the dependence of the structure factor on the order parameter μ

$$S(q, t) = Q^{-m} F(Q) \quad \text{with } Q = qR_m(t) \quad (6)$$

where $F(Q)$ denotes a scaling function[18,24] different for conserved and nonconserved order parameter models, Q is a dimensionless normalized scattering vector, and m is associated with the dimensionality of the system.

A structure factor which describes appropriately the SD process has been developed by Furukawa.[35] Schätzel and Ackerson[27,28] have used a modified expression suitable for the description of nucleation and growth which reads

$$F(Q) = \frac{27Q^2}{2(1 + 2Q^2)^3} \quad (7)$$

The early and intermediate SD stages exhibit universal behavior in many different systems, whereas the late stages of SD are system specific. In such cases, simple binary mixtures and polymers show markedly different behavior.[37,38] Although SD and nucleation are in principle different processes, there is experimental evidence suggesting a gradual transition from SD to nucleation and growth.[18−40] Due to lack of sharp distinction between unstable and metastable states, SD can be considered as a generalized nucleation theory (for a review see ref 41 and references cited therein). Finally, we should mention that the study of phase separation and spinodal type of dynamics is a subject rather rarely treated in protein literature. Most systematic experimental and theoretical studies have been undertaken by the Benedek and Tardieu groups[42−44] on eye-lens proteins.

Materials and Methods

Purity and monodispersity of lysozyme were controlled by dynamic light scattering, as previously described.[7]

Intensity distributions were recorded with a home made, 8 bit CCD apparatus previously described.[45] Records were obtained at preselected time intervals in the q range between 2.6×10^{-4} and 2.6×10^{-3} nm^{-1}. The first intensity record was taken as background and subtracted from all others records. Microscopic images of the phase separation were recorded with an Axiovert 100 inverted Zeiss microscope employing a long distance objective lens (Achrostigmat 32X, Zeiss). Samples were placed in quartz slide cells with a pathlength of 0.10 mm embedded in a massive thermostated brass holder, and the images were acquired with a CCD camera. Temperature was regulated, in both experiments, to within ±0.1 K using the Lauda RC6 and R22 thermostating and feedback units.

The CCD apparatus is placed in an air-conditioned room, and temperature quenching was accomplished by cooling the solutions from ambient to the indicated temperatures. Lysozyme and NaCl were separately dissolved in 0.10 M Na-acetate buffer, pH 4.25, at twice the indicated final concentrations, mixed and rapidly injected into 5 mm pathlength black glass cuvettes. One min was allowed for thermostating the solutions to the desired temperatures.

Results and Discussion

Observations on SD. Between 7.0 and 14.0 mM lysozyme, a phase separation is known to occur, depending on salt type, content, and temperature.[46−48] The experimental manifestation

(26) Dhont, J. K. G.; Duyndam, A. F. H.; Ackerson, B. J. *Physica A* **1992**, *189*, 503.
(27) Schätzel, K.; Ackerson, B. J. *Phys. Rev. Lett.* **1992**, *68(3)*, 337.
(28) Schätzel, K.; Ackerson, B. J. *Phys. Rev. Lett.* **1993**, *48(5)*, 3766.
(29) Allen, S. M.; Cahn, J. W. *Acta Metall.* **1979**, *27*, 1085.
(30) Lifschitz, I. M.; Slyojov, V. V. *J. Phys. Chem. Solids* **1965**, *19*, 35.
(31) Schätzel, K.; In, *Ordering and Phase Transitions*; Arora, A. K., Tata, B. V. R., Eds.; VCH Publishers: New York, 1996; p. 17
(32) Aastuen, D. J. W.; Clark, N. A.; Cotter, L. K.; Ackerson, B. J. *Phys. Rev. Lett.* **1986**, *57*, 1733; **1986**, *64*, 2772.
(33) Nikolayev, V. S.; Beysens, D.; Guenoun, P. *Phys. Rev. Lett.* **1996**, *76(17)*, 3144.
(34) Koga, T.; Kawasaki, K. *Phys. Rev. A* **1991**, *44(2)*, R817.
(35) Furukawa, H. *Physica A* **1984**, *123*, 497.
(36) Furukawa, H. *Adv. Phys.* **1985**, *34(6)*, 703.
(37) Kawakatsu, T.; Kawasaki, K.; Furukawa, M.; Okabayashi, H.; Kanaka, T. *J. Chem. Phys.* **1993**, *99*, 8200.
(38) Glotzer, S. C.; Gyuer, M. F.; Sciortino, F.; Coniglio, A.; Stanley, H. E. *Phys. Rev. E.* **1994**, *49*, 247.
(39) Guyot, P.; Simon, J. P. *J. Chimie Phys.* **1986**, *83*, 703.
(40) Binder, K. *Colloid Polym. Sci.* **1987**, *265*, 273.
(41) Koch, S. W. *Dynamics of First Order Phase Transitions in Equilibrium and Nonequilibrium Systems*; Lecture Notes in Physics, 207; Springer-Verlag: Berlin, Heidelberg, 1984.
(42) Thomson, J. A.; Schurtenberger, P.; Thurston, G. M.; Benedek, G. D. *Proc. Natl. Acad. Sci. U.S.A.* **1987**, *84*, 7079.
(43) Vérétout, F.; Delaye, M.; Tardieu, A. *J. Mol. Biol.* **1989**, *205*, 713.
(44) Liu, C.; Lomakin, A.; Thurston, G. M.; Hayden, D.; Pande, A.; Pande, J.; Ogun, O.; Asherie, N.; Benedek, G. B. *J. Phys. Chem.* **1995**, *99*, 454.
(45) Umbach, P.; Georgalis, Y.; Saenger, W. *J. Am. Chem. Soc.* **1996**, *118(39)*, 9314.
(46) Ishimoto, C.; Tanaka, T. *Phys. Rev. Lett.* **1997**, *39(8)*, 474.
(47) Phillies, G. D. J. *Phys. Rev. Lett.* **1985**, *55(12)*, 1341.
(48) Taratuta, V. G.; Holschbach, A.; Thurston, G. M.; Blankschtein, D.; Benedek, G. B. *J. Phys. Chem.* **1990**, *94*, 2140.

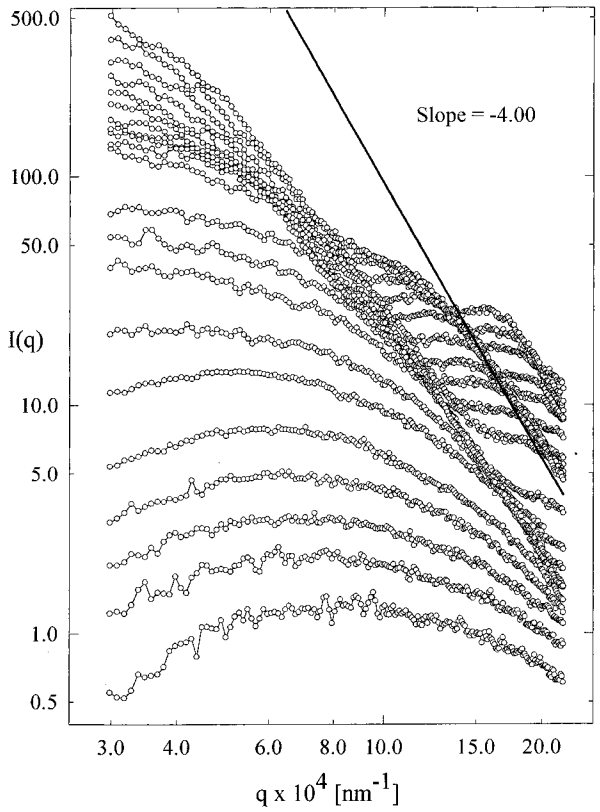

Figure 2. Typical time-resolved small-angle SLS distributions from 7.0 mM lysozyme incubated with 0.50 M NaCl in a 0.1 M Na-acetate buffer, pH 4.25 at 283.2 K following a 10 K temperature quench. Total scattered intensity, $I(q)$, plotted as a function of the scattering vector, q, in the range between 2.6×10^{-4} and 2.6×10^{-3} nm^{-1}. The slope at the wing, is -4.0, indicating evolution of globular domains with sharp boundaries. The time between records is 10 s, for clarity, above the seventh, only every second intensity value, at every third scattering vector q is shown.

of SD [It would be probably more appropriate to refer to it with some reservation using the term pseudo-SD instead. Proteins under crystallization conditions are complex systems, and extrapolations from colloids may not be directly applicable. We use here the term SD only for the sake of brevity.] presented here is, as far as we know, for the first time attempted by time-resolved small-angle SLS with a nucleating protein. Until recently, turbidity measurements have been employed instead.[49] The SD process is accompanied by a several fold increase of the scattered light intensity at forward angles, and several peaks appear in the spectra within 3 min after initializing the reaction, Figure 2. At the very early stages of the reaction, the far-field scattered intensity distribution appears as concentric rings. This behavior is typical for an SD process,[22] we display such a binary snapshot of a spinodal ring in Figure 3.

To discuss the formed microstructure at the very early stages, we need a model for explaining the domain growth. The Furukawa structure factors represented our spectra less well than the empirical structure factors predicted by Schätzel and Ackerson. We have therefore used this expression for obtaining estimates of $I_m(t)$ and $R_m(t)$. It should be noted that the latter expression is suitable for homogeneous colloidal crystallization, but its application to heterogeneous crystallization is here attempted for the first time. However, as recently shown for colloidal crystallization,[55] more exact expressions for $F(Q)$ may

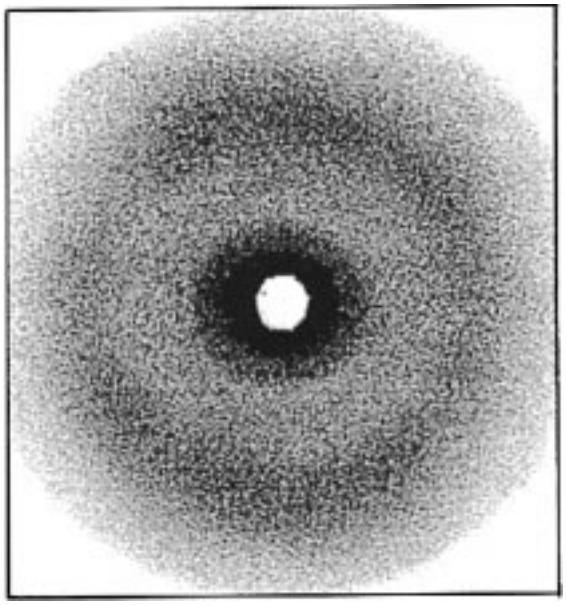

Figure 3. Far-field binary scattered intensity pattern, during an SD experiment. Conditions correspond to those of Figure 2. The central spot is a hole in the wafer that serves as a mirror, to allow for the primary laser beam to escape. The ring is not absolutely symmetric due to some flare form the walls of the light scattering cell.

require parametrization. We have used eq 7 to fit the scattered intensity distributions using nonlinear least-squares, Figure 4A. The spectra are represented well, albeit a progressive worsening of the fits occurs at larger q's. This hinders the examination of later stages and limits the number of spectra which can be evaluated with confidence. The slow penetration of the satellite peaks, Figure 2, is expected to affect the scattered intensities in the outer peak wing but not the position of the peak maximum. When appropriately scaled the records collapse practically onto a single master curve, Figure 4B, indicating dynamic scaling.

Using eqs 4 and 5 we obtain $I_m(t) \sim t^{5.10}$, Figure 5A, and $R_m(t) \sim t^{1/2}$ for the initial stages of the reaction, Figure 5B. The scaling of $R_m(t)$ suggests a diffusion-limited type of growth. The scaling exponent of $I_m(t)$, 5.10, compares favorably with the theoretically expected value of 4.0. The mean domain radii vary between 2.0 and 3.0 μm excluding appreciable sedimentation effects and the zero-time extrapolated radius of the domains is about 200 nm. The scaling properties predicted for SD appear to be valid for our system, whereby an exact scenario is by far more complex. Hydrodynamic interactions[23] and domain polydispersity effects render exact conclusions difficult.

The Transition from SD to Nucleation. At the early stages of the SD one expects a slope of -2.0 (Ornstein−Zernike exponent[50]) for the scaling of the scattered intensity in the high-q regime. This exponent approaches the -4.0 as, at later stages, distinct domains with sharp boundaries are formed. For domains with mass and surface dimensionalities d_f and d_s, the following

(49) Broide, M. L.; Tominc, T. M.; Saxowsky, M. *Phys. Rev. E* **1996**, *53(6)*, 6325.

(50) Schaefer, D. W.; Bunker, B. C.; Wilcoxon, J. P. In *Fractals in the Natural Sciences*; Fleischmann, M., Tildesley, A., Ball, R. C., Eds.; Princeton University Press: 1990; p 35.

(51) Mallamace, F.; Micali, N.; Trusso, S.; Chen, S. H. *Phys. Rev. E* **1995**, *51(6)*, 5818.

(52) Berk, N. F. *Phys. Rev. Lett.* **1987**, *58(25)*, 2718.

(53) Glatter, O.; Kratky, O. *Small Angle X-Ray Scattering*; Academic Press: London, 1982.

(54) Okada, M.; Han, C. C. *J. Chem. Phys.* **1986**, *85(9)*, 5317.

(55) He, Y.; Ackerson, B. J.; van Megen, W.; Underwood, S.; Schätzel, K. *Phys. Rev. E* **1996**, *54(5)*, 5286.

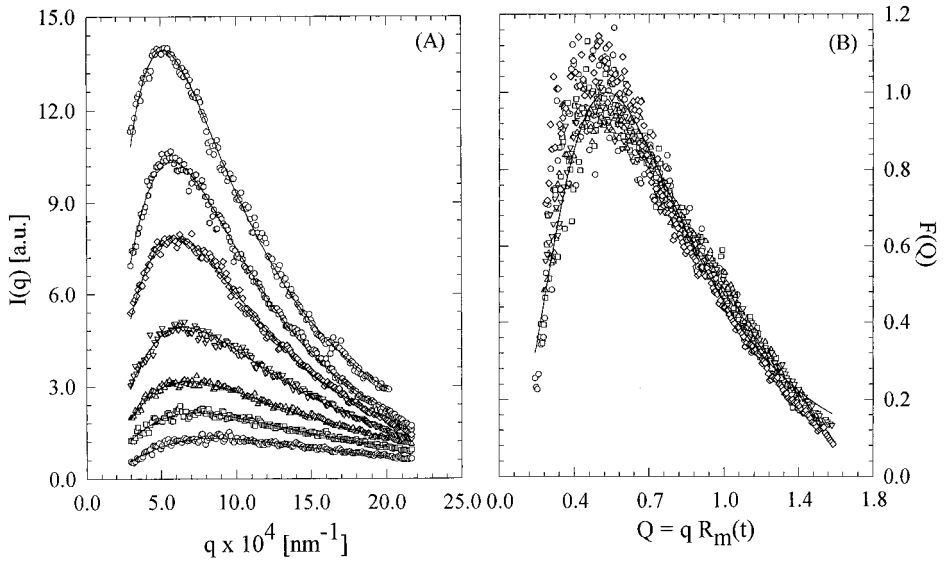

Figure 4. (A) Nonlinear least square fits on the data of Figure 2, according to eq 7 (full lines). (B) Collapse of all records on a universal master curve. The full line indicates again the fit according to eq 7.

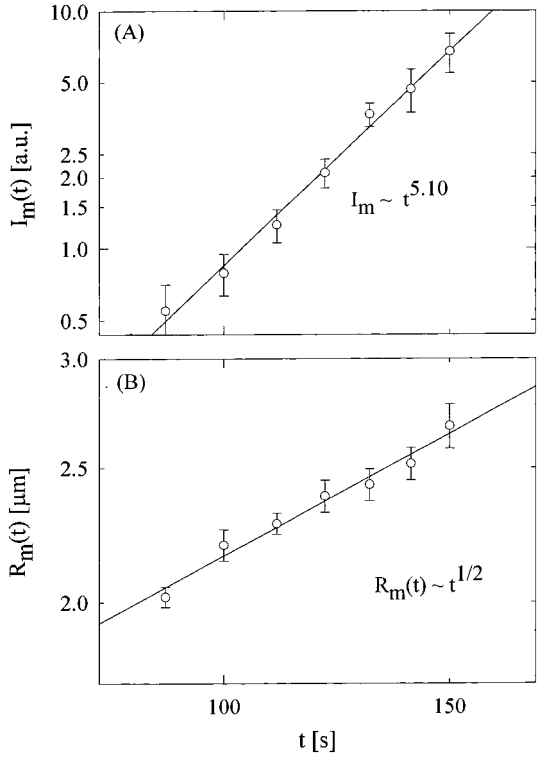

Figure 5. (A) Time evolution of the characteristic peak amplitude $I_m(t)$ (eq 4). The line indicates a slope of 5.10. (B) Time evolution of $R_m(t)$ with a slope of 1/2 (eq 5). Since there is no direct evidence of crystals being in contact or of domain walls undergoing ripening, a most probable interpretation is that domains undergo diffusion-limited growth.

scaling-law holds:

$$I(q) \propto q^{-(2d_f - d_s)} \quad \text{if} \quad qR_g \gg 1 \tag{8}$$

The high-q regime, shown in Figure 2, scales with an exponent of −4.0 (Porod-exponent[51]) indicating the evolution of globular domains, ($d_f = 3.0$) with sharp boundaries ($d_s = 2.0$). The attainment of the −4.0 slope indicates that we observe late stages of an SD process which crosses over to nucleation.[40] The satellite peaks which appear reproducibly in the intensity distributions could be attributed to higher harmonics of the basic spinodal frequency.[52] More quantitative interpretations are presently difficult due to the interactions among domains (see optical microscopy and computational sections below).

Observations on Nucleation. During nucleation the mass of the domains, proportional to the intercept at $q = 0$, increases with time. However, the surface area of the domains is proportional to d_s in the power-law regime and decreases. Therefore, the limiting slope in this regime should be equal or close to −4.0.

After the peaks have levelled-off we can still explore the events fitting the low q region of the intensity distributions with a simple Guinier[53] expression

$$I(q) = I(0) \exp\left[1 - \frac{(qR_g)^2}{3}\right] \tag{9}$$

Such fits yield values of the domain radius of gyration, R_g, and of the zero-q extrapolated scattering amplitude, $I(0)$, which is proportional to the cluster mass, as a function of time. From a series of experiments where quench depths, lysozyme, and NaCl concentrations were systematically varied, we found both $R_g(t)$ and $I(0, t)$ to fluctuate with time, Figure 6A−B, corroborating instabilities against concentration fluctuations. The domain radii varied in these experiments between 0.5 and 4 μm at the most, precluding significant gravitational effects. Similar observations of fluctuations have been made during SD in binary polymer mixtures[54] at fixed scattering angles.

When the data are plotted in a doubly-logarithmic scale we can determine approximate scaling exponents using only the initial segments of the graphs. For lysozyme−NaCl we find exponents that vary between $t^{0.40} < R_g(t) < t^{1.15}$ and $t^{1.70} < I(0, t) < t^{4.30}$. These estimates indicate a sensitive response to any change imposed to the system [The detailed description and interpretation of these experiments is beyond the scope of the present work and it will be published separately.]. At even later stages, typically above 10−20 min, we observe a rapid increment of turbidity and formation of microcrystals that indicate the onset of the liquid−solid transition. Due to multiple scattering and continuous sedimentation of microcrystals the experiments cease to provide useful information.

Microscopic Observations. The process was further studied by high resolution light microscopy. A set of microphotographs

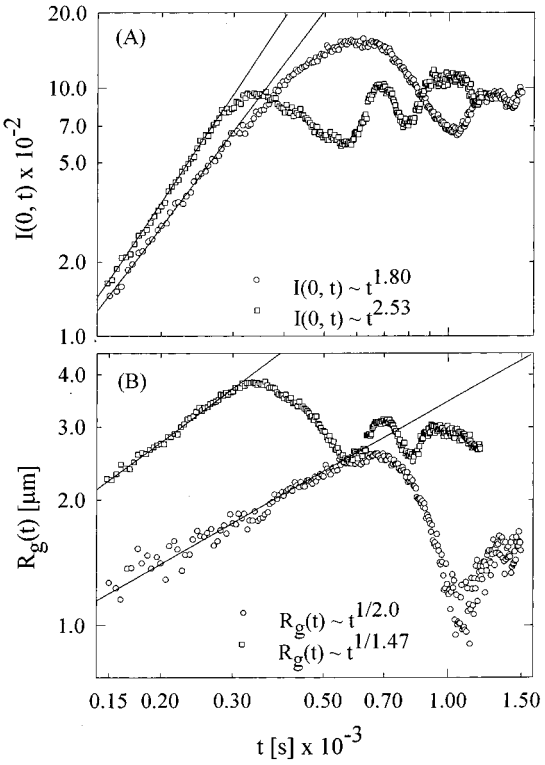

Figure 6. Evolution of (A) $I(0, t)$ and (B) $R_g(t)$ with time, at the initial nucleation stages. Conditions are 8.39 mM lysozyme incubated with 0.60 M (○) and 0.65 M (□) NaCl, in Na-acetate buffer pH 4.25, followed by an 8.5 K temperature quench to 283.2 K. Solid lines through the initial part of the curves indicate power-laws corresponding to $I(0, t) \propto t^{1.80}$ (○) and $I(0, t) \propto t^{2.53}$ (□) $R_g(t) \propto t^{1/2.00}$, (○) and $R_g(t) \propto t^{1/1.47}$ (□), respectively. Note the strong fluctuating character of both observables which, under certain conditions, persists for longer than half an hour.

of the ripening process is depicted in Figure 7A−D. At lysozyme concentrations of 13.5 mM coalescing domains, as expected for a liquid−liquid type of phase separation,[56] are formed. Especially clear coalescence was observed after 2 min, Figure 8A, with 13.5 mM lysozyme at 287.7 K. An essential feature of the observed microstructure is that it is not composed of rigid particles with fixed shape but rather of flexible domains which can assume a variety of instabilities. The most striking instability resembles a transition from globular to labyrinthine domain shapes, Figure 8B.

The domain size distribution undergoes correlated ripening as predicted by Marder[57] and will be broadened by long-time correlations (even in dilute systems) due to the continuous growth of large (critical) at costs of small (subcritical) domains. Therefore, whether a small domain will grow to a critical size or whether it will be consumed by a larger domain, depends on the average size of domains in its proximity. The time dependence of ripening depends on the spatial distribution of domains[58] and will be manifested on all observables. Even a qualitative description of these distributions is nontrivial.

The final domain shapes resemble those of modulated phases, stabilized by competing interactions if the system is near the critical regime.[59] Modulated phases may evolve in systems characterized by two or more coupled order parameters that favor different equilibrium states. By increasing the temperature

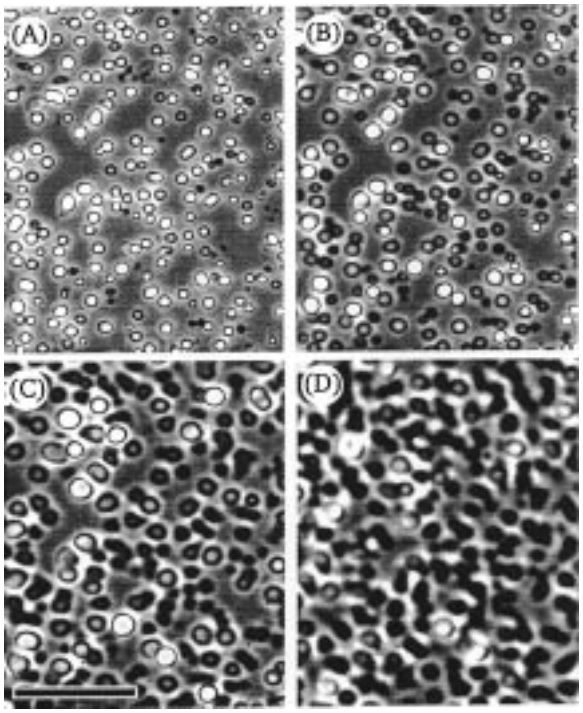

Figure 7. Evolution of coalescing domains (13.4 mM lysozyme 0.50 M NaCl in 0.10 M Na-acetate buffer, pH 4.25, and 288.0 K recorded after 20 (A), 30 (B), 40 (C), and 110 min, (D). The bar indicates 50 μm.

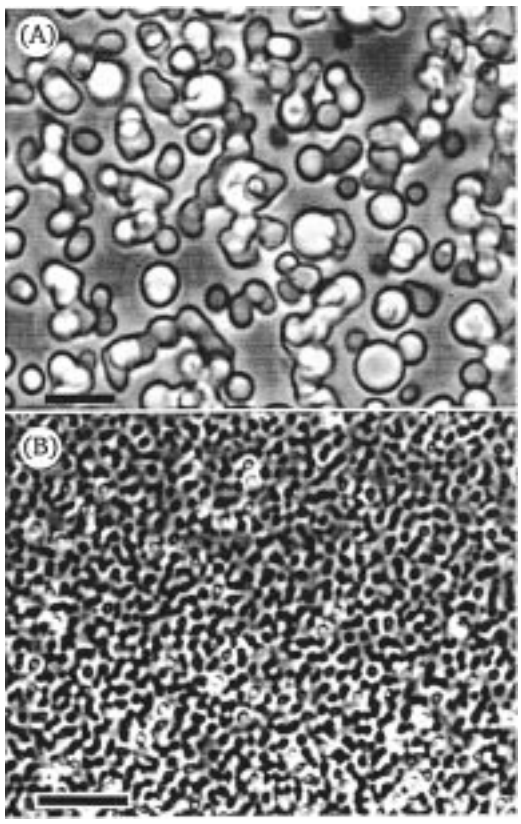

Figure 8. An especially clear picture of coalescing domains, the same conditions as in Figure 7, recorded after (A) 2 and (B) 120 min after initiating the experiment. The transition from globular to labyrinthine shapes is completed within 2 h. The bars indicate 50 μm in (A) and 100 μm in (B).

to 293.2 K the domains transform to soft crystals that gradually harden and assume the habit typical for tetragonal space group,

(56) Tanaka, H. *Phys. Rev. Lett.* **1994**, *72(11)*, 1702.
(57) Marder, M. *Phys. Rev. A* **1987**, *36(2)*, 858.
(58) Krichevsky, O.; Stavans, J. *Phys. Rev. Lett.* **1993**, *70(10)*, 1473.
(59) Seul, M.; Andelman, D. *Science* **1995**, *267*, 476.

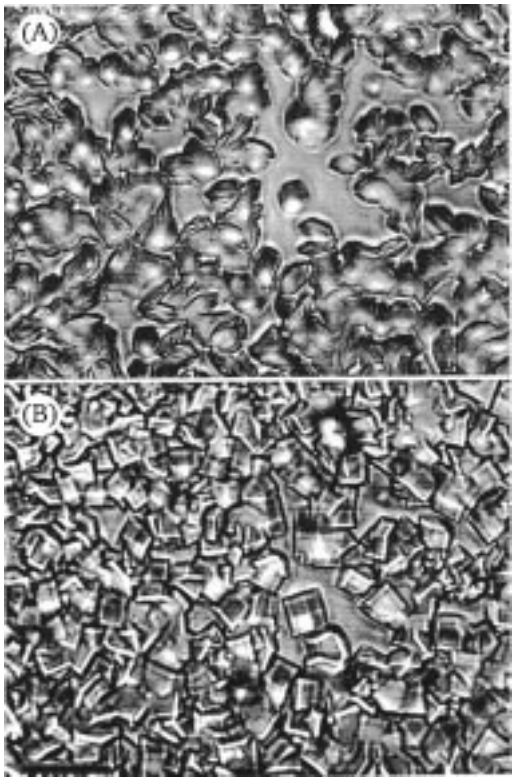

Figure 9. Gradual hardening of domains and formation of lysozyme crystals of the tetragonal group space 140 (A), and 160 min (B), after allowing the domains in Figure 7 to relax at 293 K. The bar indicates 100 μm.

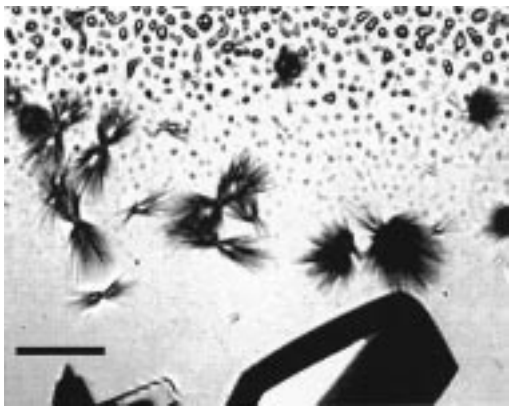

Figure 10. Selected light microscopy field showing growth of "sea-urchin" crystallites from coalescing domains under the conditions of Figure 7, 2 h after attaining maximal turbidity. The bar indicates 100 μm.

Figure 9A−B. Due to the high nucleation rates, many but very small microcrystals are formed.

Visualization of Some Temperature Induced Instabilities. We now focus on a qualitative description of instabilities observed by optical microscopic, by varying the temperature (the conditions are given in the respective pictures). The first is an instability that gives rise to "sea-urchin"-like microcrystals,[49,12] Figure 10. The second, Figure 11A−F, gives rise to cup-shaped lysozyme microcrystals. These microcrystals fuse to form typical, lysozyme crystals of tetragonal space group. This instability is, among all others, distinct and very unusual. The third observation concerns fractals growing in the proximity of lysozyme microcrystals, Figure 12A−B. The latter were recorded only close to the walls of the cell, whereas solutions

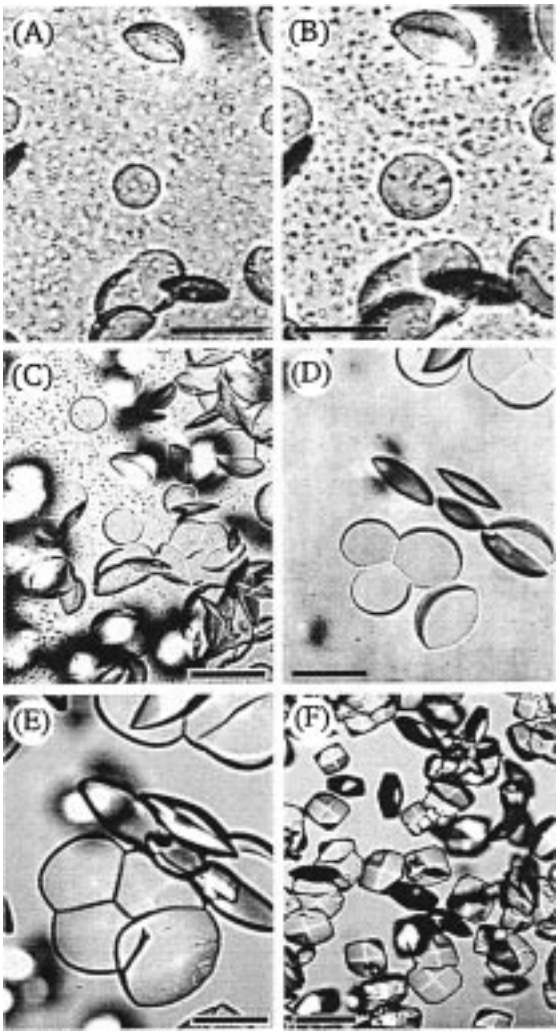

Figure 11. A peculiar instability of cup-shaped lysozyme microcrystals growing out of coalescing domains (A)−(C). Conditions are 7 mM lysozyme incubated with 0.65 M NaCl in Na-acetate pH 4.25, at 283.2 K. The bars in (A)−(E) indicate 50 and 100 μm in (F). The times between records are 10 min from (A)−(E). Complete fusion of cup-shaped microcrystals into tetragonal crystals occurs after 1 h, (F).

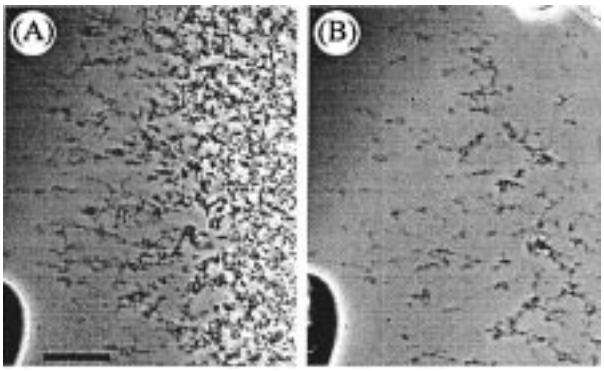

Figure 12. Fractals dissolving in the proximity of lysozyme crystals (lower left and upper right corners). Conditions are those of Figure 7, after a quench to 288.0 K. The bar indicates 100 μm. The time between recording (A) and (B) was 10 min.

were in principal void of fractal structures. Interactions with the cell walls or local temperature gradients cannot be excluded.

These observations show that multifacet microstructures may evolve in nucleating protein solutions by mere temperature variations. The differences in microstructure can be ascribed to spatial variations of the order parameter whose modulation

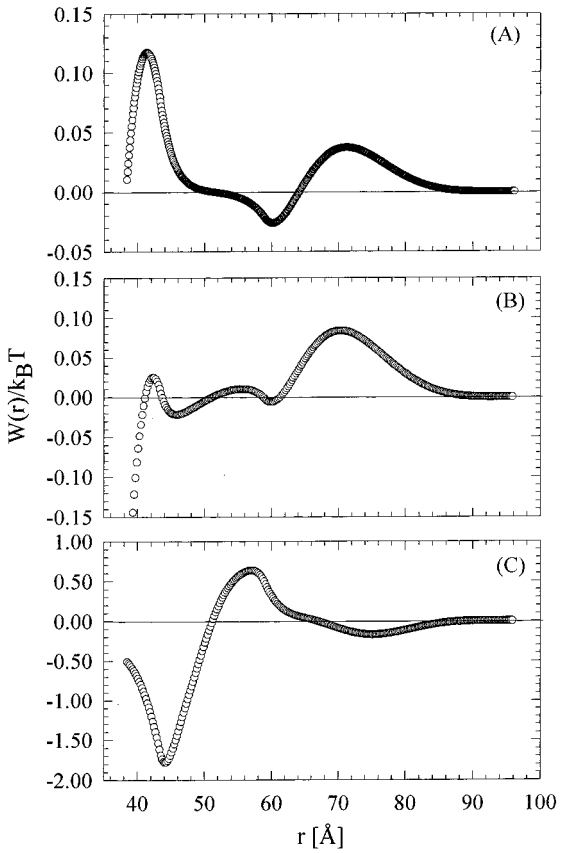

Figure 13. Potential of mean force, $W(r)/k_BT$, plotted as a function of the distance, r, between molecules for (A) 3.05, (B) 7.0, and (C) 10 mM lysozyme and 0.50 M NaCl. The repulsive barrier in (A) at 42 Å is diminished in (B) and gradually replaced by an attractive well in (C). Note the different ordinate scales of the graphs.

period depends strongly on external perturbations. A well-known example that is attributed to temperature is the space group polymorphism of lysozyme: Crystals may transform from the tetragonal to orthorhombic space group, if they grow below 318 K or above 328 K.[60]

Potential of Mean Force in the Proximity of SD. To obtain more quantitative insights concerning the effective interactions present in the system, we have recently computed the lysozyme−lysozyme potentials of mean force (PMF) for a wide range of protein and salt concentrations.[61] Lysozyme molecules were modeled as hard spheres of 38.4 Å diameter with charge $+7e$ (as observed at pH 4.25[62]). For the Na^+-Cl^- aqueous electrolyte we have used the restricted primitive model with a distance of closest approach of 4.90 Å (hydrated ions). The PMFs were obtained from numerical solutions of the coupled system of integral equations of the hypernetted chain (HNC) approach which is an excellent approximation for charged systems.[63−65] In Figure 13 we show some results relevant to the present study. As one approaches the SD region (increasing the protein concentration at fixed salt concentration), the lysozyme−lysozyme PMF undergoes drastic changes culminating in the disappearance of the 70 Å repulsive shoulder present at the lower concentrations, Figure 13A, due to collective packing effects, and the appearance of a strong attractive well (44 Å) at high lysozyme concentrations, Figure 13C. At still higher concentrations, we do not find stable solutions of the HNC equations. Although it is has been shown[66] that the HNC theory cannot localize the exact spinodal line due to its approximate nature, we believe that the behavior of the computed PMFs close to the critical region reflects to a substantial degree the true solvent mediated interactions that drive the processes here discussed.

Relations to Previous Works on Lysozyme Nucleation. The experiments described here differ drastically from previous experiments which did not employ temperature quenching. There, fractal microstructure dominated scattering, and the liquid−solid phase separation could be implied only by direct observation of lysozyme crystals after several hours or days, depending on the protein and electrolyte contents. A power-law dependence was observed to hold for both $R_g(t)$ and $I(0)$,[8] and dynamic scaling was found to hold for the aggregation kinetics of fractal microstructure when examined by dynamic light scattering and atomic force microscopy.[67] Fractal cluster growth in nucleating lysozyme solutions has been disputed by the Rosenberger group.[68,69] However, in these studies solutions were centrifuged after addition of salt and prior to the light scattering experiments. Therefore, fractals clusters were removed, and the results cannot be directly compared.[8] The experiments in the present work indicate that the domain morphology is close to spherical, and the conditions examined do not promote, at least in an obvious manner, the formation of fractal clusters as in isothermal supersaturation experiments.

Fractal formation during phase separation has been reviewed in detail by Schaefer.[50] Phase separation involving SD and nucleation is based on thermodynamics and describes adequately most observations. However, fractal structures may evolve at some stage of the phase separation, if kinetic growth processes are active. This argument is supported by computational studies on SD,[70,71] nonclassical nucleation,[72] and a series of experimental observations.[50,73] Giglio's group has also demonstrated experimentally spinodal type dynamics and ordered coarsening in colloidal fractal aggregation (see ref 74 and references cited therein).

Fractal growth is expected to cross over to the thermodynamic regimes described above. If the minority phase grows by a kinetic process, such as diffusion limited cluster−cluster aggregation, the appearance of large clusters forming from smaller ones, is not unexpected. In such a case, the scattered intensity at large-q should scale as

$$I(q) \propto q^{-d_f} \quad \text{if} \quad qR_g \gg 1 \tag{10}$$

where, for the case of diffusion limited cluster−cluster aggregation, d_f should approach the value of 1.81.[75]

(60) Takizawa, T.; Hayashi, S. *J. Phys. Soc. Jpn.* **1976**, *40(1)*, 299.
(61) Soumpasis, D. M.; Georgalis, Y. *Biophys. J.* **1997**, *27*, 2770.
(62) Eberstein, W.; Georgalis, Y.; Saenger, W. *J. Crystal Growth* **1994**, *143*, 71.
(63) Hafskøld, B.; Stell, G. In *Fluids, Simple and Complex*; Montroll, E. W., Lebowitz, J. L., Eds.; North Holland: Amsterdam, 1982; p 175.
(64) Hummer, G.; Soumpasis, D. M. *J. Chem. Phys.* **1993**, *98*, 581.
(65) Soumpasis, D. M. In *Computations of Biomolecular Structures, Achievements, Problems and Perspectives*; Soumpasis, D. M., Jovin, T., Eds.; Springer Verlag: Berlin, 1993; p 223.
(66) Belloni, L. *J. Chem. Phys.* **1993**, *99(10)*, 8080.
(67) Schaper, A.; Georgalis, Y.; Umbach, P.; Raptis, J.; Saenger, W. *J. Chem. Phys.* **1997**, *106(20)*, 8587.
(68) Muschol, M.; Rosenberger, F. *J. Chem. Phys.* **1995**, *103(24)*, 10424.
(69) Muschol, M.; Rosenberger, F. *J. Cryst. Growth* **1996**, *167*, 738.
(70) Grest, G. S.; Srolovitz, D. J. *Phys. Rev. B* **1984**, *30(9)*, 5150.
(71) Desai, R. C.; Denton, A. R. In *On Growth and Form*; Stanley, H. E., Ostrowsky, N., Eds.; Martinus Nijhoff: Dortrecht, 1986; p 237.
(72) Heerman, D. W.; Klein, W. *Phys. Rev. Lett.* **1983**, *50(14)*, 1062.
(73) Wilcoxon, J. P.; Schaefer, D. W.; Kaler, E. *Phys. Rev. Lett.* **1988**, *60(4)*, 333.
(74) Asnaghi, D.; Carpineti, M.; Giglio, M.; Vailati, A. *Physica A* **1995**, *213*, 148.

The present experiments thus raise the question whether domains, forming at very early times, and lower volume fractions via ripening, could result from or transform to fractal clusters under certain circumstances. The incorporation of nuclei to fractals, implicated in previous works,[9] may be possible if the domains do not attain the critical size which permits ripening under conditions where nonspecific attractive interactions prevail. Long times may then be required for proper alignment of nuclei to form ordered structures. In such cases, fractal aggregation could be energetically favored over nucleation.[76,77] Critical nuclei can form via restructuring of the fractal clusters similar to the observations made by Dokter et al.[78] where nucleus growth and restructuring alternate. Whereas observations involving scaling with $d_f \approx 1.8$ were typical in previous works, fractal scaling is not obvious if the experiments involve temperature quenches. This indicates that nucleation pathways may be drastically different when solutions are forced to cross into the unstable or metastable region by temperature quenching, the typical case encountered in the present work, or when clusters are subjected to shear.[79]

Some Problems Associated with These Studies

We found the temperature quenching experiments to be by far more sensitive to small changes than experiments conducted at constant temperatures. The observation of the SD process may be influenced by differences between lysozyme lots purchased either from the same or different companies. Traces of impurities, the worst of all being bound ions, which cannot be removed even by prolonged dialysis, may be present on the domain surfaces modifying their surface tension.

More stringent delivery and control system[80,81] may be helpful in future experiments to alleviate these problems. The experimental verification of the formation of submicroscopic domains of the nucleating phase in a supersaturated solution is not easy and in certain cases impossible to demonstrate. The nucleation line can be as such theoretically computed for simple systems but not necessarily measured. Some 10^3 domains in 1 cm^3 may not be detectable by light scattering or other techniques. Therefore, the observability of nucleation, especially close to critical points, is a crucial problem.[82] Nucleation events can hardly be handled reproducibly without precautions. More exact observations by time-resolved small-angle SLS are obscured by precise thermostation requirements and problems associated with controlling the speed of the reaction immediately after mixing protein and electrolyte. Stopped-flow techniques should therefore replace manual mixing operations.

Further, deeper temperature quenches and electrolytes, which shift the system through the spinodal at different temperatures, should be explored. Last, the attainment of lower scattering vectors will be required for a more precise assessment of the various SD stages. In contrast, the appearance of the satellite peaks may be better resolved by simultaneous observations at much higher q's using a separate large-angle detection unit[31,83] and higher resolution CCD devices.

Conclusions

The liquid−liquid phase transition of the system lysozyme−NaCl has been examined by time-resolved small-angle SLS and light microscopy and new aspects, relevant in understanding the complexity of protein crystallization, are introduced. They include an SD process with a peak observed at the very early stages of the reaction in the low-q regime. At later stages the SD crosses over to nucleation and liquid−solid separation.

Two factors contribute in lowering the kinetic barriers to crystallization: The undercooling in the liquid phase and the surface energy between liquid and solid phases. Their coordinated action gives rise to high nucleation rates and formation of large number of microcrystals. Nucleation occurs clearly within minutes if the solutions have been forced through the metastable region. In contrast, supersaturated solutions outside this regime nucleate after several hours or days. Very recent theoretical work[84] has shown that enhancement of protein crystal nucleation may indeed occur via critical density fluctuations. In these computations, liquid-like domains may develop toward structures with higher crystallinity at lower energy cost than that required by a direct solid−solid transformation.

Microscopic examination of the samples revealed ensembles of domains undergoing ripening and finally forming labyrinthine structures before relaxing to typical lysozyme microcrystals. Temperature induced modulations, which influence the order parameter, are responsible for the large variety of the observed instabilities. The overall behavior of the system can be qualitatively understood as correlated ripening, leading to a modulated phase type of microstructure. Computed potentials of mean force, via the hypernetted chain approximation, yield useful first insights into the effective pair interactions driving the process.

The various instabilities observed in the present work are not unexpected. The enormous complexity of microstructure emerging upon temperature and density variations has been demonstrated for micellar solutions.[16] The observed instabilities deserve quantitative explanations that can hardly be provided at present. A probable scenario could involve instabilities due to spatially variable surface tension, which set the liquid phase into motion. Temperature variations sustained by the liquid velocity may then give rise to variable surface tension which in turn promotes the different instability types.[85] Modeling of the satellite peaks, the labyrinthine modulated phases and cup-shaped microcrystals, and the theoretical distribution of domains will require extended investigations specifically devoted to these topics.

A crucial point emerging from the present and previous studies[76,77] is that detailed observations of protein nucleation events on wide spatiotemporal scales and over the phase transition plane are necessary, a task still bound to severe experimental and theoretical problems. The present work should be understood as a preliminary attempt toward comprehension of the events during protein crystallization when the latter is induced by simple electrolytes. We believe that time-resolved small-angle SLS methods can have a strong impact on capturing

(75) Klein, R.; Weitz, D. A.; Lin, M. Y.; Lindsay, H. M.; Ball, R. C.; Meakin, P. *Progr. Colloid Polym. Sci.* **1990**, *81*, 161.
(76) Georgalis, Y.; Umbach, P.; Raptis, J.; Saenger, W. *Acta Crystallogr.* **1997**, *D53*, 691.
(77) Georgalis, Y.; Umbach, P.; Raptis, J.; Saenger, W. *Acta Crystallogr.* **1997**, *D53*, 703.
(78) Dokter, W. H.; van Garderen, H. F.; Beelen, T. P. M.; van Santen, R. A.; Bras, W. *Angew. Chem.* **1995**, *107(1)*, 122.
(79) Georgalis, Y.; Umbach, P.; Zielenkiewicz, A.; Utzig, E.; Zielenkiewicz, W.; Zielenkiewicz, P.; Saenger, W. *J. Am. Chem. Soc.* **1997**, *119-(49)*, 11959.
(80) Krüger, U.; Versmold, H. *Chem.-Ing.-Tech.* **1992**, *64(2)*, 210.
(81) Palberg, T.; Härtl, W.; Wittig, U.; Versmold, H.; Würth, M.; Simmacher, E. *J. Phys. Chem.* **1992**, *96*, 8180.
(82) Goldburg, W. I. In *Light Scattering Near Phase Transitions*; Cummins, H. Z., Levanyuk, A. P., Eds.; North Holland: Amsterdam, 1983; p 531.
(83) Dhont, J. K. G.; Smits, C.; Lekkerkerker, H. N. W. *J. Colloid Interface Sci.* **1992**, *152(2)*, 386.
(84) ten Wolde, P. R.; Frenkel, D. *Science* **1997**, *227*, 1975.
(85) Siggia, E. D. *Phys. Rev. A* **1979**, *20(5)*, 595.

a plethora of events at the early stages of the nucleation reaction. The quantitative interpretation of such observations requires further experimentation supported by realistic modeling of the prevalent many body interactions.

Acknowledgment. This work was supported by grants from DFG (Sa 196/26-1) to Y.G., from DESY 05 641KEB project to P.U., and from BMBF to D. M. Soumpasis. We thank Dr. J. K. G. Dhont for forwarding us reprints of his works on SD theory and a reviewer of this journal for his constructive suggestions. Y.G. dedicates this work to the memory of Prof. Klaus Schätzel whose pioneering work has been a constant inspiration.

JA973614L